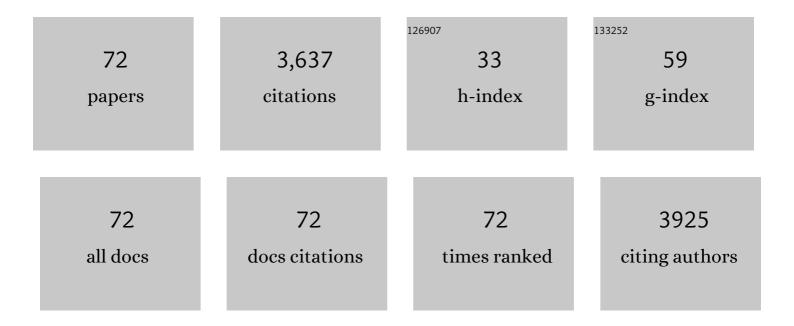
Ze-Hua Dong

List of Publications by Year in descending order

Source: https://exaly.com/author-pdf/3665535/publications.pdf Version: 2024-02-01



ZE-HUA DONC

#	Article	IF	CITATIONS
1	Advanced Architectures and Relatives of Air Electrodes in Zn–Air Batteries. Advanced Science, 2018, 5, 1700691.	11.2	645
2	Recent Progress on Transition Metal Oxides as Bifunctional Catalysts for Lithiumâ€Air and Zincâ€Air Batteries. Batteries and Supercaps, 2019, 2, 336-347.	4.7	173
3	A novel coating system with self-reparable slippery surface and active corrosion inhibition for reliable protection of Mg alloy. Chemical Engineering Journal, 2019, 373, 285-297.	12.7	168
4	N-doped carbon shell coated CoP nanocrystals encapsulated in porous N-doped carbon substrate as efficient electrocatalyst of water splitting. Carbon, 2019, 144, 464-471.	10.3	119
5	Synthesis of polypyrrole wrapped graphene hydrogels composites as supercapacitor electrodes. Electrochimica Acta, 2013, 114, 125-132.	5.2	110
6	Influence of EPS isolated from thermophilic sulphate-reducing bacteria on carbon steel corrosion. Biofouling, 2011, 27, 487-495.	2.2	106
7	Heterogeneous corrosion of mild steel under SRB-biofilm characterised by electrochemical mapping technique. Corrosion Science, 2011, 53, 2978-2987.	6.6	104
8	Graphene oxide-polythiophene derivative hybrid nanosheet for enhancing performance of supercapacitor. Journal of Power Sources, 2016, 306, 241-247.	7.8	103
9	Nitrogen-doped activated carbons derived from a co-polymer for high supercapacitor performance. Journal of Materials Chemistry A, 2014, 2, 11697-11705.	10.3	94
10	Dual nanoenzyme modified microelectrode based on carbon fiber coated with AuPd alloy nanoparticles decorated graphene quantum dots assembly for electrochemical detection in clinic cancer samples. Biosensors and Bioelectronics, 2018, 107, 153-162.	10.1	92
11	Initiation and repassivation of pitting corrosion of carbon steel in carbonated concrete pore solution. Corrosion Science, 2011, 53, 1322-1330.	6.6	91
12	The effects of Clâ^' ion concentration and relative humidity on atmospheric corrosion behaviour of PCB-Cu under adsorbed thin electrolyte layer. Corrosion Science, 2011, 53, 1230-1236.	6.6	84
13	Fabrication of superhydrophobic coating on magnesium alloy with improved corrosion resistance by combining micro-arc oxidation and cyclic assembly. Surface and Coatings Technology, 2018, 339, 155-166.	4.8	84
14	<i>In situ</i> formation of Ni ₃ Se ₄ nanorod arrays as versatile electrocatalysts for electrochemical oxidation reactions in hybrid water electrolysis. Journal of Materials Chemistry A, 2018, 6, 15653-15658.	10.3	84
15	The role of inhibitors on the repassivation of pitting corrosion of carbon steel in synthetic carbonated concrete pore solution. Electrochimica Acta, 2011, 56, 5890-5897.	5.2	78
16	Characterisation of doped polypyrrole/manganese oxide nanocomposite for supercapacitor electrodes. Materials Chemistry and Physics, 2011, 131, 529-534.	4.0	66
17	CeO2 grafted carbon nanotube via polydopamine wrapping to enhance corrosion barrier of polyurethane coating. Corrosion Science, 2021, 178, 109014.	6.6	62
18	Microstructural evolution and biological performance of Cu-incorporated TiO2 coating fabricated through one-step micro-arc oxidation. Applied Surface Science, 2020, 508, 144766.	6.1	55

ZE-HUA DONG

#	Article	IF	CITATIONS
19	Enhanced Corrosion Barrier of Microarc-Oxidized Mg Alloy by Self-Healing Superhydrophobic Silica Coating. Industrial & Engineering Chemistry Research, 2019, 58, 165-178.	3.7	53
20	Corrosion behaviour of AA6082 Al-Mg-Si alloy extrusion: Recrystallized and non-recrystallized structures. Corrosion Science, 2018, 144, 163-171.	6.6	52
21	The effects of temperature and electric field on atmospheric corrosion behaviour of PCB-Cu under absorbed thin electrolyte layer. Corrosion Science, 2011, 53, 1700-1707.	6.6	50
22	Synthesis and characterization of a bi-functional hydroxyapatite/Cu-doped TiO2 composite coating. Ceramics International, 2019, 45, 6693-6701.	4.8	48
23	Application of wire beam electrode technique to investigate the migrating behavior of corrosion inhibitors in mortar. Construction and Building Materials, 2017, 134, 167-175.	7.2	45
24	Characterization and property of dual-functional Zn-incorporated TiO2 micro-arc oxidation coatings: The influence of current density. Journal of Alloys and Compounds, 2019, 810, 151893.	5.5	43
25	Intergranular corrosion in AA2024-T3 aluminium alloy: The influence of stored energy and prediction. Corrosion Science, 2019, 155, 1-12.	6.6	43
26	Microstructure, bio-corrosion and biological property of Ag-incorporated TiO2 coatings: Influence of Ag2O contents. Ceramics International, 2019, 45, 22357-22367.	4.8	42
27	Corrosion formation and phase transformation of nickel-iron hydroxide nanosheets array for efficient water oxidation. Nano Research, 2021, 14, 4528-4533.	10.4	42
28	Growth mechanism of titania on titanium substrate during the early stage of plasma electrolytic oxidation. Surface and Coatings Technology, 2020, 400, 126202.	4.8	41
29	Formation mechanism, corrosion behaviour and biological property of hydroxyapatite/TiO2 coatings fabricated by plasma electrolytic oxidation. Surface and Coatings Technology, 2020, 386, 125483.	4.8	41
30	Polydopamine-wrapped carbon nanotubes to improve the corrosion barrier of polyurethane coating. RSC Advances, 2018, 8, 23727-23741.	3.6	38
31	Polydopamine coated prussian blue analogue derived hollow carbon nanoboxes with FeP encapsulated for hydrogen evolution. Carbon, 2019, 152, 16-23.	10.3	37
32	Synthesis, microstructure, anti-corrosion property and biological performances of Mn-incorporated Ca-P/TiO2 composite coating fabricated via micro-arc oxidation. Materials Science and Engineering C, 2020, 117, 111321.	7.3	36
33	Characterization and property of bifunctional Zn-incorporated TiO2 micro-arc oxidation coatings: The influence of different Zn sources. Ceramics International, 2019, 45, 19747-19756.	4.8	35
34	Enhanced corrosion resistance of copper by synergetic effects of silica and BTA codoped in polypyrrole film. Progress in Organic Coatings, 2019, 129, 187-198.	3.9	35
35	Microstructure, formation mechanism and antifouling property of multi-layered Cu-incorporated Al2O3 coating fabricated through plasma electrolytic oxidation. Ceramics International, 2020, 46, 2901-2909.	4.8	34
36	Weathering barrier enhancement of printed circuit board by fluorinated silica based superhydrophobic coating. Colloids and Surfaces A: Physicochemical and Engineering Aspects, 2018, 538, 628-638.	4.7	32

ZE-HUA DONG

#	Article	IF	CITATIONS
37	Monitoring of atmospheric corrosion and dewing process by interlacing copper electrode sensor. Corrosion Science, 2019, 150, 246-257.	6.6	32
38	Effect of direct current electric field on atmospheric corrosion behavior of copper under thin electrolyte layer. Corrosion Science, 2011, 53, 3446-3449.	6.6	31
39	Microbiologically influenced corrosion of X60 carbon steel in CO ₂ â€saturated oilfield flooding water. Materials and Corrosion - Werkstoffe Und Korrosion, 2013, 64, 242-246.	1.5	31
40	Integration of CoFe Alloys and Fe/Fe ₃ C Nanoparticles into N-Doped Carbon Nanosheets as Dual Catalytic Active Sites To Promote the Oxygen Electrocatalysis of Zn–Air Batteries. ACS Sustainable Chemistry and Engineering, 2020, 8, 9009-9016.	6.7	30
41	Enhanced uniformity, corrosion resistance and biological performance of Cu-incorporated TiO2 coating produced by ultrasound-auxiliary micro-arc oxidation. Applied Surface Science, 2021, 569, 150932.	6.1	30
42	Inhibition of 2-phenyl imidazoline on chloride-induced initial atmospheric corrosion of copper by quartz crystal microbalance and electrochemical impedance. Corrosion Science, 2020, 170, 108692.	6.6	29
43	Application of wire beam electrode technique to investigate initiation and propagation of rebar corrosion. Cement and Concrete Research, 2013, 48, 25-33.	11.0	27
44	Reactive incorporation of Ag into porous TiO2 coating and its influence on its microstructure, in vitro antibacterial efficacy and cytocompatibility. Progress in Natural Science: Materials International, 2021, 31, 215-229.	4.4	26
45	Degradation of fluorinated polyurethane coating under UVA and salt spray. Part I: Corrosion resistance and morphology. Progress in Organic Coatings, 2018, 123, 337-349.	3.9	25
46	Enhanced corrosion resistance of AZ31 Mg alloy by one-step formation of PEO/Mg-Al LDH composite coating. Corrosion Communications, 2022, 6, 67-83.	6.0	24
47	Microstructure, corrosion resistance, osteogenic activity and antibacterial capability of Mn-incorporated TiO2 coating. Applied Surface Science, 2020, 531, 147399.	6.1	21
48	Construction of multi-layered Zn-modified TiO2 coating by ultrasound-auxiliary micro-arc oxidation: Microstructure and biological property. Materials Science and Engineering C, 2021, 131, 112487.	7.3	20
49	Microstructural characterization and in vitro biological performances of Ag, Zn co-incorporated TiO2 coating. Ceramics International, 2020, 46, 29160-29172.	4.8	19
50	Enhancement of Corrosion Resistance and Biological Performances of Cu-Incorporated Hydroxyapatite/TiO ₂ Coating by Adjusting Cu Chemical Configuration and Hydroxyapatite Contents. ACS Applied Bio Materials, 2021, 4, 903-917.	4.6	19
51	Degradation of fluorinated polyurethane coating under UVA and salt spray. Part âj: Molecular structures and depth profile. Progress in Organic Coatings, 2018, 124, 25-32.	3.9	18
52	Ag distribution and corrosion behaviour of the plasma electrolytic oxidized antibacterial Mg-Ag alloy. Electrochimica Acta, 2022, 411, 140089.	5.2	16
53	PEO coating on Mg-Ag alloy: The incorporation and release of Ag species. Journal of Magnesium and Alloys, 2023, 11, 2182-2195.	11.9	15
54	Microstructure and Corrosion Resistance of Plasma Electrolytic Oxidized Recycled Mg Alloy. Acta Metallurgica Sinica (English Letters), 2022, 35, 961-974.	2.9	13

ZE-HUA DONG

#	Article	IF	CITATIONS
55	A pH-responsive cerium-imidazole decorated ZIF-8 to achieve self-healing barrier property for epoxy coating on Al alloy by controlled release. Progress in Organic Coatings, 2022, 163, 106640.	3.9	13
56	The corrosion behavior of carbon steel in CO ₂ â€saturated NaCl crevice solution containing acetic acid. Materials and Corrosion - Werkstoffe Und Korrosion, 2012, 63, 720-728.	1.5	12
57	Impedance sensor for the early failure diagnosis of organic coatings. Journal of Coatings Technology Research, 2018, 15, 1259-1272.	2.5	12
58	Investigation on initial atmospheric corrosion of copper and inhibition performance of 2-phenyl imidazoline based on electrical resistance sensors. Materials Chemistry and Physics, 2021, 262, 124321.	4.0	12
59	Corrosion behviour of micro-arc oxidized titanium in NaCl solution with H2O2 and albumin. Materials Chemistry and Physics, 2022, 276, 125376.	4.0	11
60	The synergistic effect of Ag and ZnO on the microstructure, corrosion resistance and in vitro biological performance of titania coating. Surface and Coatings Technology, 2021, 426, 127798.	4.8	11
61	Simultaneous tuning of the cation content and pore structure of cobalt-iron bimetal phosphide to enhance the electrochemical oxygen evolution. Journal of Alloys and Compounds, 2020, 842, 155784.	5.5	9
62	Effects of temperature on polarity reversal of under deposit corrosion of mild steel in oilfield produced water. Corrosion Engineering Science and Technology, 2020, 55, 708-720.	1.4	9
63	A chemically robust and self-healing superhydrophobic polybenzoxazine coating without fluorocarbon resin modification: Fabrication and failure mechanism. Progress in Organic Coatings, 2022, 163, 106630.	3.9	9
64	Comparative investigation on copper atmospheric corrosion by electrochemical impedance and electrical resistance sensors. Transactions of Nonferrous Metals Society of China, 2021, 31, 3024-3038.	4.2	9
65	Investigation on the initial atmospheric corrosion of mild steel in a simulated environment of industrial coastland by thin electrical resistance and electrochemical sensors. Corrosion Science, 2022, 204, 110389.	6.6	9
66	The Influence of Stored Energy on Grain Boundary Chemistry and Intergranular Corrosion Development in AA2024-T3 Alloy. Materials, 2018, 11, 2299.	2.9	6
67	Microstructure, anti-corrosion and biological performance of Ag, Zn Co-doped titania coating: The influence of Zn contents. Ceramics International, 2021, 47, 11129-11143.	4.8	5
68	The influence of room temperature storage on intergranular corrosion susceptibility of AA6082 Al-Mg-Si alloy. Corrosion Communications, 2021, 3, 71-79.	6.0	5
69	Preventing surface passivation of transition metal nanoparticles in oxygen electrocatalyst to extend the lifespan of Zn-air battery. Journal of Materials Science and Technology, 2022, 128, 205-212.	10.7	5
70	Early identification of stress corrosion cracking of P110 low alloy steel in downhole fluid by electrochemical noise measurement. Corrosion Engineering Science and Technology, 2021, 56, 230-243.	1.4	3
71	Synergistic inhibition of cerium and alkyl phosphate composite adlayer on pitting corrosion of Al–Mg–Si aluminium alloy. Corrosion Engineering Science and Technology, 2021, 56, 678-689.	1.4	3
72	One-pot synthesis and microstructure of multi-layered nanospheres via plasma electrolytic oxidation. Ceramics International, 2021, 47, 28037-28041.	4.8	3